# Synthesis, characterization and catalytic application of MgO supported metal catalysts in synthesis of dihydropyrimidinone

**Tushar Shamba Anvekar*, Kanika K. Korgaonkar and Hari Kadam**
Department of Chemistry, St. Xavier's College, Mapusa, Goa – 403507, India
tsanvekar@yahoo.co.in

## Abstract

*In the present investigation, syntheses of different metal supported MgO catalysts have been envisaged. Samples have been prepared by two different ways viz.; (a) Sol-gel self propagating low temperature combustion method for synthesis of Ni/MgO, Co/MgO and Ru/MgO catalysts and (b) Impregnation method for synthesis of 20% Ni/MgO and 20% Co/MgO catalysts samples were characterized using instrumental techniques such as XRD, SEM, FT-IR, BET analysis. XRD data reveals that samples possess particle size of 8.420 nm and 17.439 nm at 2 Θ values of 43.137 and 49.955 respectively. The SEM micrographs shows that the particles possesses irregular shape and are generally random, non-uniform manner with particle size approximately <100 nm . All the catalysts supported on MgO are found as amorphous in nature. The IR spectra gives fundamental band for Mg-O at 1384 cm$^{-1}$ and for Mg –O stretching at 911 cm$^{-1}$ confirms the formation of MgO support. The BET analysis depicts the surface area of 91.1 m$^2$/gm with pore radius of 2.12 nm. The adsorption isotherm follows the micro porous structure of the prepared samples. The catalytic activity of the Ni/Mgo and Co/MgO has been investigated for the Biginelli reaction for synthesis of dihydropyrimidinone. The supported catalysts were found to be active for synthesis of dihydropyrimidinone. Co/MgO supported catalyst gave better yield (> 60 %) as compared to Ni /MgO support.*

**Keywords**: Supported catalyst, Dihydropyrimidinone, Catalytic activity.

## Introduction

Catalysts demonstrate diverse roles in furnishing the society with fuels, pharmaceuticals, fine chemicals while maintaining safety and clean environment. Broadly classified as Homogeneous or Heterogeneous catalysts, latter has a different phase than the reactants. Mostly Heterogeneous catalysts are solid in nature and act on liquid or gaseous substrates. Supported Heterogeneous catalysts are in recent times gaining popularity wherein the active catalyst is dispersed on another support material that enhance its effectiveness[1-4].

The important characteristics features of the support are: Surface area**:** The active phase of the catalyst is dispersed on the surface of the supports. Thermal stability: In general, for most of the catalytic and non-catalytic reactions to take place, they have to surmount the activation barrier. Prevention of agglomeration: Since the temperature increases during the course of the reaction, the particles of active species can migrate over the support and can coalesce to form bigger particles. Magnesium oxide (MgO) is widely selected as a catalyst support because of its high thermal stability[5-12].

## Materials and methods

**Sol-gel self propagating low temperature combustion method:** Catalyst M/MgO (M=Ni, Co, Ru) was synthesised by the sol-gel self propagating low temperature combustion process. AR grade reagents were used in all the synthesis. Calculated amount of Ni(NO$_3$)$_2$.6H$_2$O, Co(NO$_3$)$_2$.6H$_2$O, RuCl$_3$ and Mg(NO$_3$)$_2$. 6H$_2$O in the molar ratio of M/Mg of 2:1 and of nitrate or chloride salt / ascorbic acid of 1:1 were mixed (30 min) and fully dissolved in a given amount of de-ionized water. Then the mixture was stirred for 1 h at < 100$^o$C (on hotplate) in order to remove water until a gel like products were formed. Then, foam like product was further formed by heating it in a big evaporating dish at a temperature between 250$^o$C – 300$^o$C which further leads to form a grey–black M/MgO precursor powder. The final powdered product was then calcined for 12 h at 500$^o$C[13-15].

**Impregnation method:** The desired amount of MgO (commercial) powder was added into de-ionized water under vigorous stirring forming slurry (solution 1). In another beaker, a required amount of metal salts [Ni(NO$_3$)$_2$.6H$_2$O and Co(NO$_3$)$_2$.6H$_2$O] dissolved in de-ionized water (solution 2). solution 2 was added drop wise into the water slurry of MgO i.e. solution 1 and stirring was kept for 15 min after the addition. The resulting slurry of MgO with nitrate salt solution was subsequently heated on a hotplate at 80$^o$C for 35 min to vaporize the excessive water. The wet solid obtained was dried at 110$^o$C for 4 h. Finally, the dried sample was calcined at 500$^o$C for 12 h in a muffle furnace forming a grey-black product (m = 20%, M$_{0.2}$Mg$_{0.8}$O$_2$)[16-18].

**Characterization:** Powder X-ray diffraction (XRD) pattern of the prepared catalyst were obtained from Philips X'Pert Pro diffractometer using Ni filtered Cu Kα radiation (λ= 1.5418 A°) operated at 40kV and 40mA over a 2θ range of 10°-80°. The identification of compounds in powder samples was attained by comparison of the peaks with data files provided by Joint Committee on Powder Diffraction Standards (JCPDS). Crystallite size for intense peak was determined using the Debye-Scrrer equation, $D = 0.9\lambda/\beta Cos\theta$, where $\theta$ is the diffraction angle, $\beta$ is full width at half maximum and dspacing was also calculated by using Bragg's law, $d = n\ \lambda/2\sin\theta$. Followed by the calculation for lattice parameter $(a) = d (h^2 + k^2 + l^2)^{1/2}$. Surface morphology of the samples was investigated by Scanning Electron Microscope (SEM, JEOL JSM – 6360LV). Fourier Transform Infrared (FTIR) specta were recorded on Thermo Fischer FTIR instrument in the range of 4000 cm$^{-1}$ to 400 cm$^{-1}$. The samples were analyzed after being mixed with KBr. The nitrogen adsorption/desorption isotherms were determined at 77 K using BELSORP MINI II catalysts were degassed at 673 K for 3 h at vacuum pressure of 10$^{-2}$ kPa. Specific Surface Area (SSA) of the calcined samples were calculated by Brunauer-Emmett-Teller (BET) method and the meso-pore size distribution was obtained by the Barret-Joyner-Halenda (BJH) method[19].

**Catalytic application: The Biginelli Reaction:** A solution of benzaldehyde (10 mmol, 1.06g), ethylaceto acetate (13 mmol,

1.69g) and urea (15 mmol, 0.90g) was heated to reflux (85°C-90°C) in ethanol in the presence of MgO supported catalyst (0.2g) for 3 h (Scheme-1). On completion of reaction, the mixture was filtered to separate the catalyst and the filtrate was collected ina beaker containing crushed ice. Then, the crude product formed was collected by filtration and was re-crystallized using ethyl acetate. The synthesized compound has been identified by comparison of spectral data (IR) and melting point (mp) with that reported[20-24].

## Results and discussion

In this study, MgO supported catalyst were prepared namely; Ni/MgO, 20% Ni/MgO, Co/MgO, 20%Co/MgO and Ru/MgO.

**Specific surface area (BET):** Table-1 describes the specific area of prepared catalysts. MgO catalyst support has high surface area and nanocrystalline structure. The specific surface area (SSA) as well as pore distribution size was found better for Ni/MgO catalysts as compared to Co/MgO. The N$_2$ adsorption isotherm for the calcined MgO catalysts are shown in Figure-1 (a) and 1 (b). This is a type IV isotherm with a hysteresis loop indicating agglomeration of particles with non-uniform size and shape. The meso pore size distribution of samples as shown in Figure-1 (c) and 1 (d) has pore radius in the range of 2-8 nm. Results also infer that Ni/MgO had more SSA than Co/MgO.
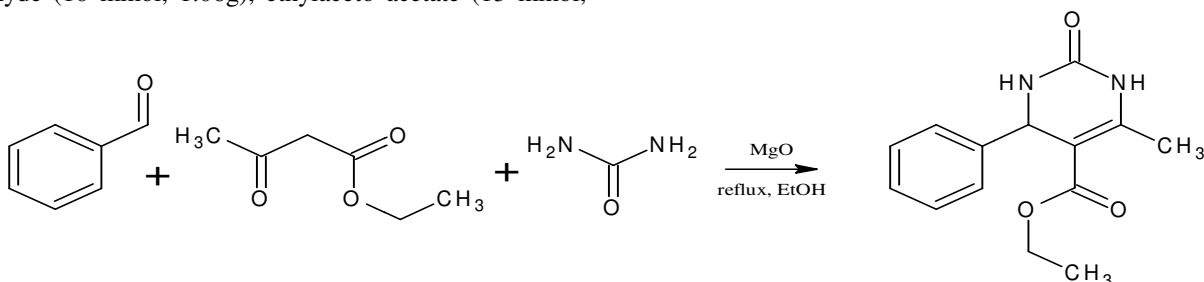


**Scheme-1:** The Biginelli reaction.

**Table-1:** Surface area and mesopore structure of supported catalysts.

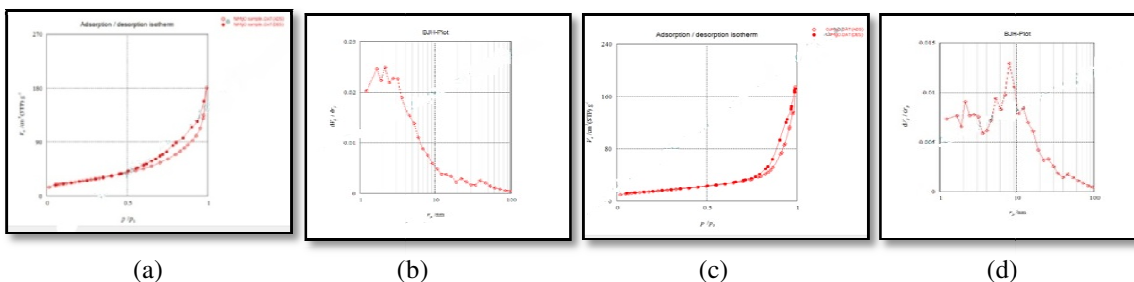| Catalyst | BET area (m$^2$/g) | Pore specific surface area (m$^2$/g) | Pore volume (cm$^3$/g) | Pore radius (nm) |
|---|---|---|---|---|
| Ni/MgO | 91.9 | 94.5 | 0.269 | 2.12 |
| Co/MgO | 54.46 | 54.2 | 0.255 | 7.94 |



| (a) | (b) | (c) | (d) |

**Figure-1**: N$_2$ adsorption isotherm (a and c) and meso pore size distributions (b and d) of the calcined MgO catalysts.

**5.2 X-ray Diffraction (XRD):** Figure-2 depicts the XRD patterns of the calcined samples of Ni/MgO catalysts, where the diffraction peaks of the samples was indexed by comparison to data given in JCPDS 24-0712 card for Ni/MgO. The lattice parameter a = 4.186 Å and 4.2034 Å are in good agreement with the standard (4.2123Å-4.1773Å) [3]. The diffraction peaks at $2\theta$ = 36.9°, 42.9°, 62.9°, 75° and 79° corresponding to (111), (200), (220), (311) and (222) planes respectively. These peaks might be attributed to MgO and NiO. As NiO and MgO have similar crystal structure, their XRD peaks are seen to overlap. The crystalline size of Ni/MgO and 20% Ni/MgO was calculated for the intense peak using Debye-Scherrer equation and was found to be 8.420 nm and 17.439 nm, respectively.
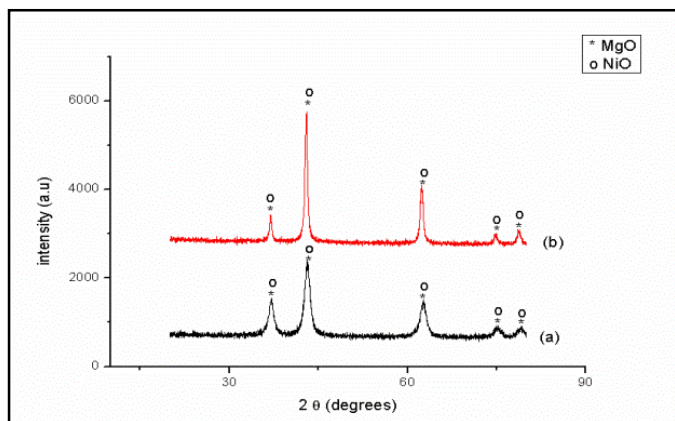


**Figure-2**: Combined graph of Ni/MgO catalyst (a) Ni/MgO prepared by combustion method and (b) 20% Ni/MgO prepared by impregnation method calcined at 500°C.

Figure-3 shows the XRD patterns of the calcined samples of Co/MgO catalysts, where the diffraction peaks of the samples was identified by consulting to data given in JCPDS 78-0430 card. The lattice parameter a = 4.109 Å and 4.219 Å are in good agreement with the standard. The diffraction peaks at $2\theta$ = 36.9°, 42.9° and 62.9° corresponds to (111), (200) and (220) planes, respectively. These peaks might be attributed to MgO and CoO. The crystalline size of Co/MgO and 20% Co/MgO was found to be 7.124 nm and 14.893 nm, respectively.
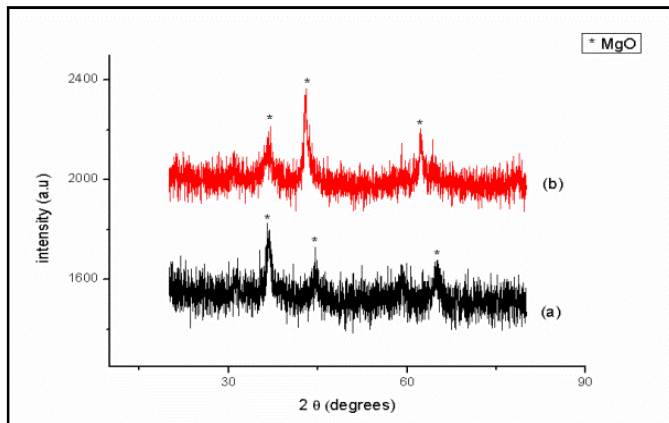


**Figure-3:** Combined graph of Co/MgO catalyst (a) Co/MgO prepared by combustion method and (b) 20% Co/MgO prepared by impregnation method calcined at 500°C.

**Scanning electron microscopy (SEM):** This study was employed in an attempt to identify the presence of crystalline of metals on the surface, their size and dispersion. Figure-4 shows the sample structure has been formed of irregular shaped small particles. The particles are generally in random and non-uniform manner with approximately <100 nm particles size. All the catalysts supported on MgO are found as amorphous in nature[25].

**Fourier Transfer Infrared Spectroscopy (FT-IR):** Table-2 summarized the characteristics band peaks for different prepared MgO supported catalysts. The broad vibration band at 3426 -3432 cm$^{-1}$ represents Mg-OH and -OH stretching vibration of surface hydroxyl group and absorbed water molecules. This is due to the adsorption of water molecules onto support when it is exposed to atmosphere. While at 2920 cm$^{-1}$ range it shows C-H stretching. Around 1400cm$^{-1}$, it shows Mg-O stretching vibration. In the lower regions (1000–400 cm$^{-1}$), bands due to Mg-O bonds or Metal-O bonds appears. A broad band stretching vibration mode for Mg-O-Mg is observed at 480-600 cm$^{-1}$ [25].

Figure-5 shows the spectra for different synthesized M/MgO supported catalysts.
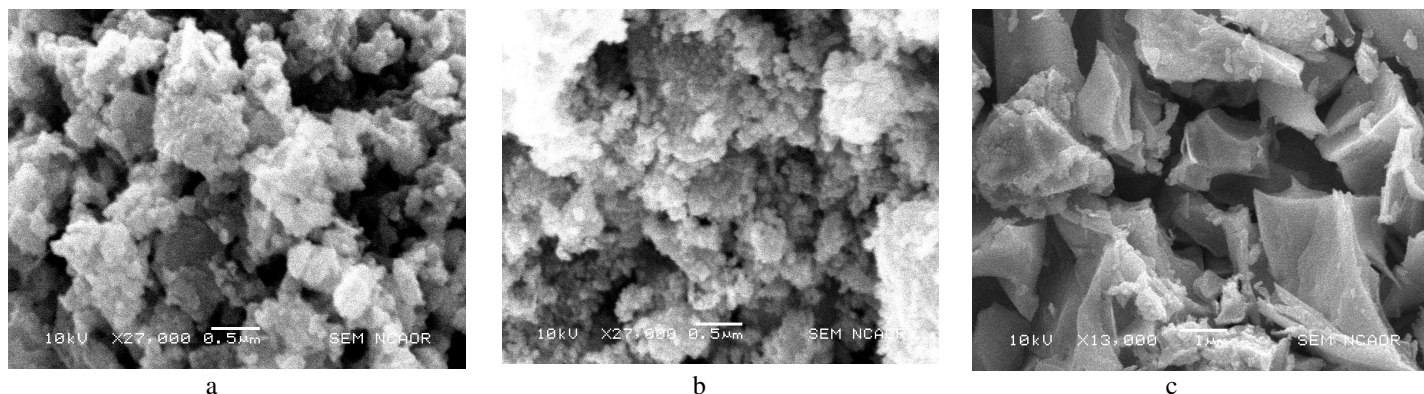


**Figure 4:** SEM image for (a) Ni/MgO, (b) Co/MgO and (c) Ru/MgO catalyst calcined at 500°C.

**Table-2:** Characteristic band peaks for different MgO supported catalyst.

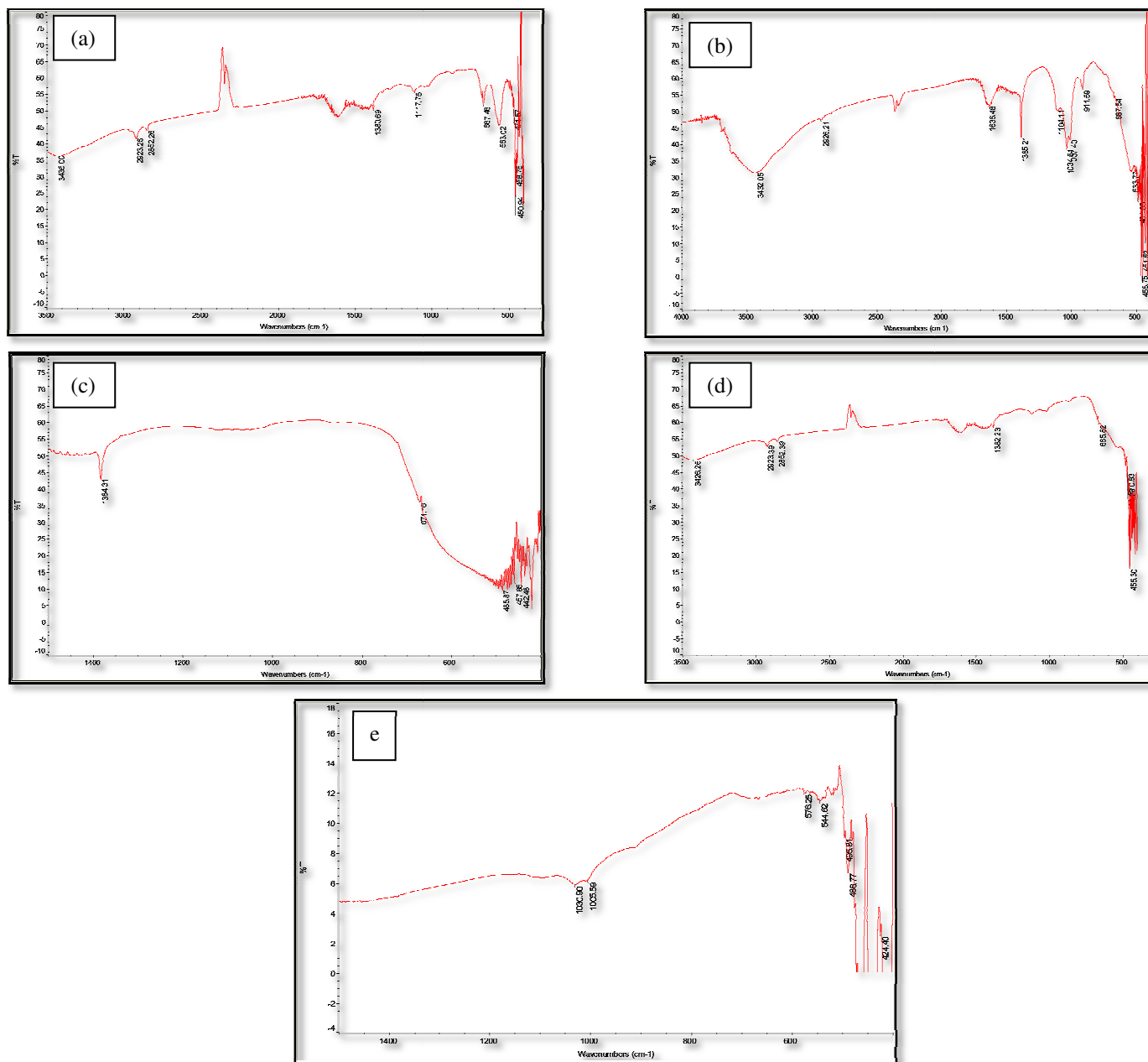| Observed bands (cm$^{-1}$) | | | | | Stretching |
|---|---|---|---|---|---|
| Ni/MgO | 20%Ni/MgO | Co/MgO | 20%Co/MgO | Ru/MgO | |
| 3432.05 | - | 3435.00 | 3426.26 | - | O-H stretch |
| 2926.21 | - | 2923.25 | 2923.39 | - | C-H stretch |
| 1385.21 | 1384.31 | 1380.69 | 1382.23 | - | Mg-O bond |
| 911.59, 677, 533,481,451 | 671, 485, 457, 442 | 1117,667,563, 471, 458, 450 | 665, 456 | 1030.90 – 424.40 | M-O bond stretch |



**Figure-5:** FT-IR spectra of M/MgO (a) Ni/MgO, (b) 20% Ni/MgO, (c) Co/MgO, (d) 20%Co/MgO and   (e) Ru/MgO
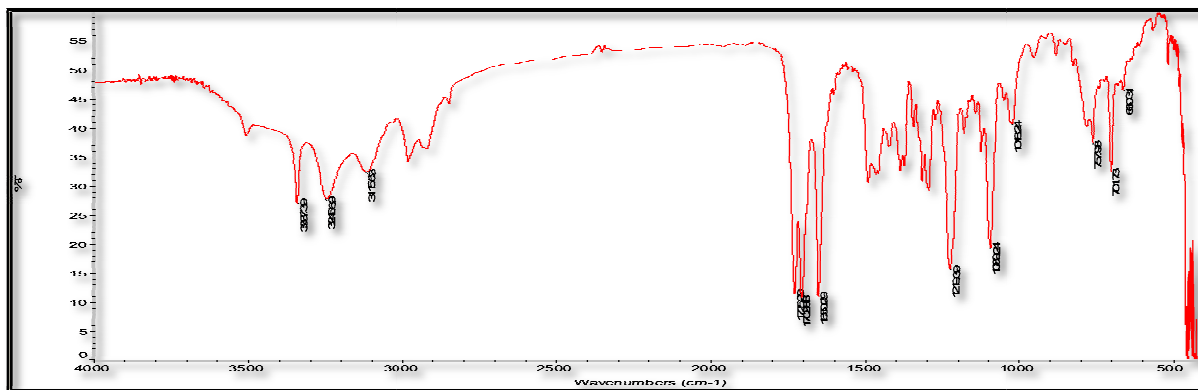
**Figure-6:** FT-IR spectra of dihydropyrimidinone.

**Catalytic activity:** In this work we report an efficient three-component, one-pot synthesis of dihydropyrimidinone derivative in the presence of three different supported magnesium oxide (MgO) catalyst such as commercially available, Ni/MgO, Co/MgO and Ru/MgO as a effective heterogeneneous base catalyst. The melting point was found to be 207°C and was matching with the reported melting point[20-24].

Table-3 gives the yield (in percentage) obtained for the performed Biginelli reaction for the dihydropyrimidinone product. Also, Figure-6 shows the spectra for the dihydropyrimidinone product confirming its formation while Table-4 gives its characteristics band peaks.

**Table-3:** Yield (%) for dihydropyrimidinone product

| Catalyst | Time (min) | Yield (%) |
|---|---|---|
| Commercial MgO (0.2g) | 180 | 32 |
| Ni/MgO (0.2g) | 180 | 61.73 |
| Co/MgO (0.2g) | 180 | 65.76 |
| Ru/MgO (0.1g) | 180 | 11.42 |

**Table-4:** Characteristics band peaks for dihydropyrimidinone spectra

| Observed peaks (cm-1) | Type of Stretching |
|---|---|
| 3337.39 | N-H stretch |
| 3115.53 | N-H stretch |
| 2979.46 | C-H stretch |
| 1725.29 | C=O ester stretch |
| 1702.88 | C=O amide stretch |
| 1650.29 | C=C str. |
| 1089.21 | Monosubstitued aromatic ring |

## Conclusion

In conclusion, MgO supported catalysts prepared by the sol-gel self propagating low temperature combustion method calcined at 500°C presented efficient yield in synthesis of dihydripyrimidinone. Ascorbic acid used in sol-gel self propagating self combustion method acted as fuel in the synthesis of catalyst. In impregnation method, the catalyst exhibit poor activities due to surface sintering and poor distribution of the active oxygen species. Co/MgO supported catalyst gave better yield (> 60 %) as compared to Ni /MgO support.

## Acknowledgements

## References

1. Andache M., Rezaei M. and Moghadam M.K. (2013). A nanocrystalline MgO support for Ni catalysts for steam reforming of $CH_4$. *Chinese Journal of catalysts,* 34(7), 1443-1448.

2. Zhang Y., Tang Y.H., Zhang E.L., Lin L.W. and Pei L.Z. (2010). Preparation of Ni/MgO catalysts for carbon nanofibres by a self-propagating low temperature combustion process. *Materials Science-Poland*, 28(4), 805-815.

3. Zhang M., Ma H. and Gao Z. (2015). Phase composition of $Ni/Mg_{1-x}Ni_xO$ as a catalyst prepared for selective methanation of CO in $H_2$-rich gas. *Journal of nanomaterials*, 16(1), 1-10. Article ID790857, 1-10. http://dx.doi.org/10.1155/2015/790857

4. Hu S., Xue M., Chen H. and Shen J. (2010). The effect of surface acidic and basic properties on the hydrogenation of aromatic rings over the supported nickel catalysts. *Chemical Engineering Journal*, 162(1), 371-379.

5. Wen G., Xu Y., Xu Z. and Tian Z. (2009). Characterization and catalytic properties of the Ni/$Al_2O_3$ catalysts for aqueous-phase reforming of glucose. *Catalyts letter*, 129(1), 250-257.

6. Garcia S.R. and Assaf J.M. (2012). Effect of the preparation method on Co/$Al_2O_3$ catalyst applied to ethanol steam reforming reaction production of hydrogen. *Modern Research in Catalysis*, 1(3), 52-57.

7. Abudukelimu N., Xi H., Gao Z., Zhang Y., Ma Y., Mamat X. and Eli W. (2015). Preparation and characterisation of Ru/$Al_2O_3$ catalysts by adsorption-precipitation-activation method and selective hydrogenation of Dimethyl maleate to Dimethyl Succcinate. *Material Science and Engineering with Advanced Research.,* 1(1), 31-37.

8. Lopez T., Garcia-Cruz I. and Gomez R. (1994). Spectroscopic study of Pt/MgO catalysts prepared by the sol-gel method. *Materials Chemistry and Physics*, 36(3-4), 222-230.

9. Jianwen D. and Shikong S. (2000). Effects of preparation method on the catalytic properties of Ba/MgO catalyst in oxidation coupling of methane. *Journal of Natural Gas Chemistry*, 9(3), 231-236.

10. Babaie M. and Sheibani H. (2011). Nanosized magnesium oxide as a highly effective heterogeneous base catalyst for the rapid synthesis of pyranopyrazoles via a tandem four-component reaction. *Arabian Journal of Chemistry*, 4(2), 159-162.

11. Mohammadzadeh I., Bavafa M. and Sheibani H. (2013). A Fast One-Pot Multi-Component Synthesis Of 3,4-Dihydropyrimidin-2(1h)-ones In The Presence Of Magnesium Oxide As A Highly Effective Heterogeneous Base Catalyst. *Revue Roumaine De Chimie*, 58(9-10), 773-777.

12. Zare A., Hasaninejad A., Khalafi-Nezhad A., Ahmad R., Moosavi Z. and Abolfath P. (2007). Organic reactions in ionic liquids: MgO as efficient and reusable catalyst for the Michael addition of sulfonamides to α,β-unsaturated esters under microwave irradiation. *ARKIVOC* , 13, 105-115.

13. Phucho I.T., Nongpiur A., Tumtin S., Nongrum R. and Nongkhlaw R.L. (2009). Recent progress in the chemistry of dihydropyrimidinones. *Rasayan Journal Chem.*, 2(3), 662-676.

14. Jagir S.S. (2012). Past, present and future of the Biginelli reaction: a critical Perspective. *ARKIVOC,* 66-133.

15. Wagh M.S., Patil A.M., Baviskar H. and Wagh M.M. (2015). Preparation Of MgO Nanostructure Powder By Sol-Gel Method. *International Journal of Chemical and Physical Sciences* (IJCPS), 4, 115-117.

16. Viswanathan B. (2009). Catalysis: Selected Applications. Alpha Science.

17. Wen G., Xu Y., Ma H., Xu Z. and Tian Z. (2008). Production of hydrogen by aqueous-phase reforming of glycerol. *International Journal of Hydrogen Energy,* 33(22), 6657-6666.

18. Shaaban E.R., Kaid M.A. and Ali M.G.S. (2014). Xray analysis and optical properties of nickel oxide thin films. *Journal of Alloys and Compounds*, 613, 324-329.

19. Fateme M., Rezaei M., Fereshteh M. and Zohreh F. (2015). Carbon dioxide reforming of methane for syngas production over Co–MgO mixed oxide nanocatalysts. *Journal of Industrial and Engineering Chemistry*, 21, 662-667.

20. Qu H., Li X., Mo F. and Lin X. (2013). Efficient synthesis of dihydropyrimidinones via a three-component Biginelli-type reaction of urea, alkylaldehyde and arylaldehyde. *Beilstein J. Org. Chem.*, 9(1), 2846–2851.

21. Peng J. and Deng Y. (2001). Ionic liquids catalyzed Biginelli reaction under solvent-free Conditions. *Tetrahedron Letters,* 42(34), 5917–5919.

22. Oliver Kappe C. (2000). Recent Advances in the Biginelli Dihydropyrimidine Synthesis. New Tricks from an Old Dog. *Acc. Chem. Res.*, 33(12), 879-888.

23. Sahu P.K., Lal J., Thavaselvam D. and Agarwal D.D. (2012). A facile green synthesis and in vitro antimicrobial activity 4H-pyrimido [2,1-b] [1,3] benzothiazole derivatives using aluminum trichloride under solvent free conditions. *Medicinal Chemistry Research,* 21(11), 3826–3834.

24. Vasconcelos A., Oliveira P.S., Ritter M., Freitag R.A., Romano R.L., Quina F., Pizzuti L., Pereira C., Francieli M.S. and Alethéa G.B. (2012). Antioxidant capacity and environmentally friendly synthesis of dihydropyrimidin-(2H)-ones promoted by naturally occurring organic acids. *Journal of Biochemical and Molecular Toxicology,* 26(4), 155-161.

25. Hu Yun H. (2010). Advances in Catalysts for $CO_2$ Reforming of Methane. *ACS Symposium Series*, 155-174.

26. Zhiming G., Lin C. and Hongwei M. (2016). Selective methanation of CO over Ni/$Al_2O_3$ catalyst: Effects of preparation method and Ru addition. *International Journal of Hydrogen Energy*, 41(12), 5484-5493.